Published in final edited form as:
Behav Brain Res. 2011 January 1; 216(1): 36–45. doi:10.1016/j.bbr.2010.06.032.

Somatosensory and Sensorimotor Consequences Associated with the Heterozygous Disruption of the Autism Candidate Gene, *Gabrb3*

Timothy M. DeLorey[1], **Peyman Sahbaie**[1], **Ezzat Hashemi**[1], **Wen-Wu Li**[2], **Ahmad Salehi**[3], and **J. David Clark**[2,4]

[1]Molecular Research Institute, Palo Alto, CA 94303, USA

[2]Veterans Affairs Palo Alto Health Care System, Palo Alto, CA 94304, USA

[3]Department of Neurology, Stanford University School of Medicine, Palo Alto, CA 94305, USA

[4]Department of Anesthesiology, Stanford University School of Medicine, Palo Alto, CA 94305, USA

Abstract

Autism spectrum disorder (ASD) is diagnosed based on three core features: impaired social interactions, deficits in communication and repetitive or restricted behavioral patterns. Against this backdrop, abnormal sensory processing receives little attention despite its prevalence and the impact it exerts on the core diagnostic features. Understanding the source of these sensory abnormalities is paramount to developing intervention strategies aimed at maximizing the coping ability of those with ASD. Consequently, we chose to examine whether sensory abnormalities were present in mice heterozygous for the *Gabrb3* gene, a gene strongly associated with ASD. Mice were assessed for tactile and heat sensitivity, sensorimotor competence (accelerating rotarod task) and sensorimotor gating by prepulse inhibition of the acoustic startle reflex (PPI). All heterozygotes exhibited an increase in seizure susceptibility and similar reductions in *Gabrb3* expression in the dorsal root ganglia, spinal cord, whole brain and amygdala. Interestingly, significant differences were noted between heterozygous variants in regards to tactile sensitivity, heat sensitivity, sensorimotor competence and PPI along with differences in *Gabrb3* expression in the reticular thalamic nucleus and the bed nucleus of stria terminalis. These differences were influenced by the heterozygotes' gender and whether the *Gabrb3* gene was of paternal or maternal origin. These results are not adequately explained by simple haploinsufficiency of *Gabrb3*, therefore, additional mechanisms are likely to be involved. In addition, this is the first report of the occurrence of tactile and heat hypersensitivity in an ASD mouse model, two features often associated with ASD.

Keywords

Gabrb3; GABA; Sensorimotor gating; Tactile hypersensitivity; Heat hypersensitivity; Sensory processing; Reticular thalamic nucleus; Bed nucleus of stria terminalis; Autism spectrum disorder

Corresponding author: Timothy M. DeLorey, Ph.D., Molecular Research Institute, P.O. Box 51687, Palo Alto, CA 94303, Tel: 650-269-9805, Tim@molres.org.

Introduction

$GABA_A$ receptors are ligand-gated chloride channels that play a critical role in neurodevelopment and mediate most of the fast synaptic inhibition in adult brain. Functional $GABA_A$ receptors are constructed from a pool of heterogeneous subunits that assemble together to form multiple subtypes that exhibit differing GABA sensitivities and pharmacologies [4, 50]. The β_3 subunit, encoded by the GABRB3 gene, is the major β isoform present during brain development and is strongly implicated in ASD [1, 59, 61]. Although no one gene will be universally responsible for all idiopathic cases of autism, two recent studies of postmortem ASD brain found that the majority of brains studied displayed significant reductions in the expression of the β_3 subunit protein [15, 59]. Moreover, the first direct evidence of *GABRB3* involvement in ASD, due to a nucleotide coding variant of *GABRB3*, was recently reported by Delahanty et al. [9].

The prevalence of autism spectrum disorder (ASD) has been estimated to be as high as 1 out of 91 children [34] with a 4:1 male to female ratio [18]. The core diagnostic traits of ASD include impaired social interactions, stereotypical or restrictive behaviors, and communication deficits [21]. However, a number of other behavioral abnormalities are common to ASD, including hyperactivity, epilepsy, sensorimotor deficits, sleep disturbances and sensory processing abnormalities in auditory, visual, tactile and thermal modalities [6, 33, 57]. Although sensory processing abnormalities are common to ASD they manifest in diverse ways, in a study of 200 cases of ASD about 39% showed hypo-responsiveness, 19% hyper-responsiveness and 36% displayed mixed responsiveness [23].

Although mice lacking the *Gabrb3* gene (*Gabrb3*−/−) exhibit a number of abnormalities relevant to ASD [10, 12, 65], mice with a heterozygous deletion of the *Gabrb3* gene are likely to be a more accurate representation of the molecular constituency of ASD. However, to date *Gabrb3* heterozygous mice have not been typically reported as having significant behavioral abnormalities. These observations may be, in part, due to the unusually high behavioral variability displayed by heterozygous mice [11, 38, 65] that were of a mixed-strain background, C57BL/6J × 129Sv/SvJ, two substrains commonly reported as being behaviorally different [30, 44]. To avoid such confounds we backcrossed the *Gabrb3* gene disruption for seven generations against pure C57BL/6J, largely reducing the 129Sv/SvJ contribution. We hypothesized that haploinsufficiency of *Gabrb3* expression, on a stable background, would be sufficient to alter behaviors often associated with ASD such as abnormalities in somatosensory processing and sensorimotor function. In this report, behavioral assessments were done in conjunction with measurements of *Gabrb3* expression levels in several neural components associated with the assessed behaviors.

Materials and Methods

Techniques used to disrupt the *Gabrb3* gene have been previously described [29]. Mice with a heterozygous disruption of the *Gabrb3* gene, were originally obtained from Dr. Gregg Homanics at University of Pittsburgh, PA. These mice are now available from the Jackson Laboratory (Bar Harbor, ME). The mouse line used in the current study was backcrossed for seven generations against the background C57BL/6J strain. The nomenclature used throughout this manuscript identifies heterozygous mice (p/m) as containing a disrupted (−) or intact (+) *Gabrb3* gene on the paternal allele (p) or maternal allele (m). Therefore, a p−/m + designation indicates that the mouse has a disrupted *Gabrb3* gene on the paternal allele and an intact *Gabrb3* gene on the maternal allele. Mice were evaluated between 10–36 weeks of age, within a weight range of 19–32 g. Two cohorts were used in this study, the first completed the following series of behavioral experiments in the same order (tactile, heat, wire test, marble burying and lastly seizure susceptibility) with one week between each

set of behavioral tasks. A second cohort underwent rotarod testing followed a week later by startle and PPI evaluation. Throughout the study heterozygous mice were gender matched to littermate controls. Mice were housed in groups of 3–5 on a 12/12-h light/dark cycle (lights on at 06:00 hours) in a climate-controlled room with food and water provided *ad libitum*. Genotyping was conducted by PCR on tail tissue samples. All animal protocols conformed to the guidelines determined by the National Institute of Health (USA) Office for Protection from Research Risks and were approved by the Animal Care and Use Committee of the Veterans Affairs Palo Alto Health Care System. Assessments were made relative to gender and whether the disrupted gene was of paternal or maternal origin. In all behavioral assays the evaluators were blinded to the genotypes of the mice being tested.

Behavioral Assays

Mechanical Threshold—Static tactile allodynia (tactile hypersensitivity) is predominantly mediated by Aδ fibers and can be detected by a heightened response to the application of small, stiff probes (i.e. von Frey monofilaments) to the skin of humans or the hindpaws of rodents [17, 48]. The assessment of mechanical (tactile) sensitivity was determined according to the "up-down" method described by Chaplan et al. [7]. Briefly, a series of Semmes-Weinstein calibrated von Frey monofilaments (Stoelting Co., Wood Dale, IL) were used, with nine filament strengths chosen at logarithmic intervals, ranging from 0.04 to 4 g. Mice were allowed to acclimate for 30 min within a nonrestrictive Plexiglas cylindrical enclosures (diameter 10 cm and height 30 cm) placed on top of a wire-mesh surface elevated 40 cm above the table's surface. After the adaptation period the smallest diameter filament was applied to the center of the plantar surface of the hind paw. The stimulus was applied for 5 sec with enough force to bend the fiber slightly with withdrawal of the hind paw from the fiber scored as a response. When no response was observed, the next stiffest fiber in the series was applied to the same paw. If a response was obtained, a less stiff fiber was applied, if no response occurred the next stiffer fiber was once again applied. Testing proceeded in this manner until four fibers, after the one that elicited the first response, were applied. Mechanical withdrawal thresholds were calculated using a data fitting algorithm of the response data, which permitted the use of parametric statistics for comparison analysis [55].

Heat Sensitivity—In order to determine whether heterozygous mice exhibited a change in sensitivity to heat, the method of Hargreaves, modified for use in mice, was employed to assess heat hyperalgesia [25]. Mice were allowed to acclimate for 30 min in nonrestrictive Plexiglas enclosures (10 cm diameter × 30 cm height) placed on a clear glass plate maintained at 29oC. A radiant heat source was activated in conjunction with a timer and focused onto the planter surface of the hind paw. When the paw was withdrawn, both heat and timer were halted. The radiant heat intensity was adjusted to provide approximately a 10 sec paw withdrawal baseline for control mice (+/+), this setting was used in all subsequent experiments. A maximal cut-off of 20 sec was used to prevent tissue damage. Four measurements were made per animal per test session.

Acoustic startle and prepulse inhibition—The methods used for assessing acoustic startle, a primitive brainstem reflex, and prepulse inhibition (PPI), a phenomenon in which a weak pre-stimulus reduces the startle response to subsequent startling stimulus, were adapted from Frankland et al., [19]. Startle testing was conducted using a SR-Lab startle response system (San Diego Instruments, San Diego, CA). Mice were placed in a nonrestrictive Plexiglas cylinder (3.2 cm internal diameter) resting on the sensor platform within the ventilated apparatus. A piezoelectric accelerometer, attached to the base of the sensor platform, detected and transduced all mouse movements, which were digitized and stored by computer. Acoustic startle stimuli, prepulse stimuli and the continuous background

white noise of 65 decibels (dB) were delivered via a high-frequency speaker (frequency range of 0.4–16 kHz) located 28 cm above the containment cylinder. The speakers, containment cylinder and sensor platform were housed within a sound-attenuated chamber. The startle amplitude was taken to be the maximal response that occurred within 65 msec of the presentation of the startle stimulus (recorded every msec). The sound levels for background noise and startle/prepulse stimuli were verified with a digital sound level meter, and the SR-Lab calibration unit was used routinely to ensure uniform sensitivity between test chambers.

Following an acclimation period of 5 min within the containment cylinder, mice were exposed to an acoustic startle stimuli at each of five different startle stimulus intensities (80, 90, 100, 110, 120 dB) with the startle reflex amplitude being recorded and stored via computer interface. PPI was evaluated by the presentation of a non-startling acoustic prepulse just prior to a startling stimulus with measurements reflecting the percentage inhibition of the normal startle amplitude that occurred in the absence of the prepulse. Each PPI trial consisted of a startle stimulus (120 dB, 40 msec), which was preceded by a prepulse of 70, 80 or 90 dB with a fixed interval (100 msec) between onsets of the prepulse and startle stimuli. A prepulse was 20 msec in duration with a rise/fall time of less than 1 msec. Each trial was presented once in a pseudo-random sequence within each test session block with a variable inter-trial interval (ITI) of 12–30 sec (average 15 sec). A total of 10 trial blocks for each startle and PPI session were presented. The following formula was used to calculate % prepulse inhibition of a startle response: % PPI= 100 − [(startle response with prepulse presented before the startle stimulus/startle stimulus response alone) × 100].

Accelerating Rotarod—In the accelerating rotarod task, a mouse is required to constantly make postural adjustments in order to maintain balance on the rotarod and avoid falling off. The rotarod (Smartrod Model SRTC, AccuScan Instruments, Columbus, OH) consists of a 10-cm-diameter rubber-coated cylinder that can revolve at varying speeds. Each trial was started by placing a mouse on the stationary rod for 30 sec to acclimate, followed by the rod being accelerated from 3 to 19 rpm over a 180 sec period. Each mouse received one trial per day for seven consecutive days. Latency time to fall off the accelerating rotarod was recorded automatically by the Smartrod.

Marble burying—The marble burying procedure has been reported to assess obsessive-compulsive tendencies as well as repetitive/perseverative responses in mice [63, 67]. The marble burying procedure used was adapted, with minor modifications, from previous studies [67]. Briefly, mice were acclimated to the testing room for 1 hr prior to test chamber adaptation (Day 1) and prior to testing (Day 2). During adaptation, each animal was individually acclimated for 30 min to the clear polypropylene testing chamber (13 cm × 20 cm × 30 cm) containing a 5 cm deep layer of sawdust bedding. On day 2, mice were individually placed back into the test chamber, which now contained 24 clear glass marbles (one cm in diameter) placed in six rows of four, on top of a 5 cm deep layer of sawdust. The number of marbles fully buried in 30 min was recorded.

Wire hanging test—The wire hanging test is a simple approach used to measure neuromuscular ability (muscle tone and grip strength) of a rodent by assessing the animal's ability to hang suspended by its forepaws from a wire (2 mm diameter) 30 cm above a sawdust covered surface for a maximum time of 1 min [32, 49]. Latency to fall was measured from the time a mouse was placed hanging by its forepaws on the wire until it fell. The test was performed twice for each mouse with results from each mouse being averaged and data analyzed.

Pentylenetetrazol (PTZ) induced seizures—PTZ induced seizure sensitivity experiments were conducted using a minimal number of animals. A sub-convulsant dose of PTZ (35 mg/kg) in 0.9% sodium chloride solution was administered via intra-peritoneal (i.p.) injection. Mice were scored using the seizure scoring method of Schwaller et al., [60]. Specifically, seizures were scored as follows: 1) behavioral arrest and staring, 2) whole body twitching or mild tremor, 3) myoclonic jerking of the head and forelimbs numbering less than 20, 4) myoclonic jerking of the head and forelimbs number more than 20, 5) bilateral forelimb clonus 6) generalized tonic-clonic seizures, often involving wild running and jumping behavior with loss of postural control, 7) status epilepticus defined as 10 min or more of continuous or closely spaced seizures with no return to normal behavior, often resulting in death. All sessions were videotaped for 30 min and scored by two blinded observers.

Collection of dorsal root ganglia (DRG), spinal cord and whole brain—Mice were sacrificed by CO_2 inhalation. The posterior elements of the spine were removed and the segmental nerves were cut immediately distal to the ganglion using spring scissors and whole spinal cord removed and placed in 4°C RNA Later buffer (Ambion Austin, TX) followed by RNA extraction. To remove lumbar DRGs (L1–L6) the dorsal root was gently tugged to pull the DRG into the vertebral canal, then nerves were clipped and connective tissue removed prior to DRG removal. Although removal of the spinal cord improves access to DRGs, care was taken to minimize the amount of nerve collected with the ganglia. Lumbar DRGs were collected using a dissection microscope (Model 570, AO Instrument Co., Buffalo, NY) and transferred to Eppendorf tubes kept on dry ice and then stored at −80°C until used. The whole brain was removed from the skull and placed in 4°C RNA Later buffer (Ambion Austin, TX) followed by RNA extraction.

Laser Capture Microdissection (LCM)

Preparation—Mice were exposed to CO_2 for 30 sec and perfused transcardially with 20 ml phosphate buffered saline (0.1 M) in diethyl pyrocarbonate (DEPC) treated water. The brains were removed and embedded in Optimal Cutting Temperature (OCT) compound (Triangle Biomedical Sciences, Durham, NC) and kept at −80°C until used.

Coronal sections (20 μm thick) were prepared using a cryostat microtome (Leica CM 1850, Houston, TX), collected onto membrane slides (Molecular Machines & Industries Inc., Haslett, MI), and stored at −80°C. Tissue slides were fixed, processed and stained as follows, 70% ethanol for 30 sec followed by DEPC-treated water for 5 sec, stained for 30 sec with 0.5% toluidine blue and washed in DEPC-treated water for 1 min. Subsequent dehydration of slides was accomplished using a series of increasing alcohol solutions (50% – 100%) for 30 sec each and lastly placed in xylenes for 2 min [66].

The Laser Microdissection System MMI version 2.3 (Molecular Machines & Industries Inc., Haslett, MI) with settings of speed 37%, focus 46% and energy 99% was used to dissect out the reticular thalamic nucleus (RTN) (bregma −0.46 to −1.70 mm), bed nucleus of stria terminalis, (supracapsular part) (BNST) (bregma −0.58 to −1.34 mm) and the amygdala (basolateral nucleus (anterior part) and the lateral nucleus) (bregma −0.70 to −1.46 mm) from the coronal sections [51]. A total area of 100–200 μm^2 was taken from 2–3 sections from each mouse using a 4x or 10x objective. The collected samples were placed on a diffusor cap of a LCM plastic collection tube (Molecular Machines & Industries Inc. Haslett, MI) and immediately stored at −80°C until mRNA extraction.

RNA extraction and cDNA synthesis—Whole brain, spinal cord and DRG tissue samples were homogenized in TRI Reagent (1 ml per 100 mg of tissue) (Sigma, St. Louis,

MO) using a Polytron homogenizer for brain and Pyrex glass/glass homogenizer for spinal cord and DRG tissue. Total RNA was extracted according to manufacturer guidelines. Briefly, homogenized tissue samples were allowed to stand for five min at room temperature. Subsequently, 0.2 ml chloroform, per ml of TRI Reagent, was added to the sample and shaken vigorously for 30 s followed by 10 min incubation at room temperature. Samples were centrifuged at 12,000× *g* for 15 min at 4°C. The upper phase (300–450 μl) was transferred to a fresh Eppendorf tube. Room temperature isopropyl alcohol (0.5 ml per 1 ml TRI Reagent)was added and allowed to sit for 10 min in order to precipitate the total RNA. This was followed by centrifugation at 12,000 × *g* for 15 min at 4°C. The resulting RNA pellets were washed with 1 ml 75% ethanol. Total RNA was dissolved in RNase-free water and kept at −80°C until used. Total RNA isolation from LCM samples, including DNase treatment, were performed using the RNAqueous-Micro kit (Ambion, Austin, TX) according to the manufacturer's instructions and stored at −80°C until used.

RNA was reverse transcribed to cDNA using the High Capacity cDNA Reverse Transcription Kit (Applied Biosystems, Foster City, CA). The reverse transcription reaction was performed at 25°C for 10 min, 37°C for 120 min, and 85°C for 5 sec. The cDNA was stored at −20°C until used in RT-PCR.

Quantitative Real-Time PCR (RT-RCR)—A volume of 20 μl of cDNA from DRG and spinal cord was diluted 1:10 with sterile water and used as the template while 20 μl of the cDNA from brain tissues was diluted 1:20 with sterile water and used as the template. Quantitative RT-PCR was performed using the SYBR Green PCR master kit (Applied Biosystems, Foster City, CA). In brief, RT-PCR amplification mixtures contained 2.5μl template cDNA, 2x SYBR Green I Master Mix buffer (2.7μl) and 0.3μl forward and reverse primers (2.5 pmol). The cycling conditions included 10 min polymerase activation step at 95°C and then 40 cycles of 95°C for 15 sec followed by 60°C for 60 sec. All PCR reactions were done in triplicate. Relative quantitation of data obtained from the ABI PRISM 7700 Sequence Detection System was performed using the comparative method. The amount of target expressed in the spinal cord and DRG was normalized to an endogenous reference housekeeping gene for hypoxanthinephophoribosyltransferase (*Hprt*). The amount of target expressed in brain was normalized to an endogenous reference housekeeping gene for β-actin. The primers used in the real-timePCR were as follows:

Forward primer for *Hprt*: 5′-GCTTGCTGGTGAAAAGGACCTCTCGAAG-3′

Reverse primer: 5′-CCCTGAAGTACTCATTATAGTCAAGGGCAT-3′, PCR product size: 117 bp.

Forward primer β-actin: 5′-GGCTGGCCGGGACCTGACAGACTAC-3′

Reverse primer: 5′-GCAGTGGCCATCTCCTGCTCGAAGTC-3′, PCR product size: 150 bp.

Forward primer *Gabrb3* (Exon 4): 5′-AGTGAAAAACCGCATGATCC-3′

Reverse primer (Exon 5): 5′-GCAGTTTTGCTCATCCAGTG-3′, PCR product size: 121 bp.

Primers were designed using software from Integrated DNA Technologies (http://www.idtdna.com).

Monitoring the real-time increase in fluorescence of SYBR-Green dye provided a means for semi-quantitative analysis of the data. All data were normalized to the *Hprt* or β-actin mRNA threshold cycle (CT) level and then relative to a calibrator (reference sample placed on each plate) and expressed as mRNA relative fold change.

Statistical analysis—Data were analyzed for statistical significance using Prism 4.03 software (GraphPad, San Diego, CA) with a value of $p<0.05$ being considered statistically significant. One-way ANOVA with Tukey's *post hoc* multiple comparison tests were used to determine the level of significant differences between genotypes and their respective gender-matched controls in the tactile and heat sensitivity experiments as well as in the marble burying and wire hanging experiments. The data from the acoustic startle stimulus were analyzed using a two-way ANOVA with pairwise comparisons at each acoustic intensity performed *post hoc* using unpaired two-tailed *t* tests. PPI data were statistically analyzed using a two-way ANOVA with *post hoc* pairwise comparisons using Bonferroni tests. Rotarod data were analyzed by two-way repeated measures ANOVA with pairwise comparisons for each trial day performed using unpaired two-tailed *t* tests. In the PTZ experiments, significant differences were determined by a nonparametric Kruskal-Wallis test followed by a Mann-Whitney *U* test. Expression of the *Gabrb3* gene in heterozygous and control mice were compared using Kruskal-Wallis test followed by a Mann-Whitney *U* test.

Results

Breeding

Mating between female heterozygotes and male C57BL/6J mice produced percentages of offspring that were in accordance with what would be predicted by Mendelian genetics, roughly 48% +/+ and 52% +/−. However, mating between male heterozygotes and female C57BL/6J mice produced slightly skewed percentages of 58% +/+ and 42% +/−. Although, little can be made of such results, it suggests p−/m+ heterozygotes may experience a slightly higher mortality rate prior to weaning than p+/m− heterozygotes.

Mechanical Threshold

Upon application of von Frey filaments to the hind-paw, wildtype (+/+) mice displayed withdrawal thresholds of 1.63 ± 0.24 g for females (n=14) and 1.44 ± 0.12 g for males (n=15). Female heterozygotes of both genotype distinctions displayed a trend towards lower paw withdrawal thresholds than controls but genotype differences were found to be non-significant ($F_{2,45}=2.46$, $p=0.10$) (Fig 1). However, between male genotypes, differences were found to be significant ($F_{2,38}=23.20$, $p<0.001$), suggesting an increase in mechanical responsiveness (Fig 1). *Post hoc* analysis revealed significant differences between controls and p+/m− and p−/m+ male mice ($p<0.05$ and $p<0.001$, respectively). In addition, male p−/m+ mice were found to be significantly more responsive to innocuous mechanical stimuli than were male p+/m− mice ($p<0.01$) (Fig. 1).

Heat Sensitivity

Assessment of Hargreaves heat sensitivity revealed mean baseline paw withdrawal latencies for female +/+ mice (n=7) of 9.8 ± 0.2 sec and for male +/+ mice (n=7) of 9.2 ± 0.4 sec. Genotype differences were found to be significant in paw withdrawal latencies amongst female ($F_{2,18}=7.9$, $p<0.01$) and male ($F_{2,18}=21.4$, $p<0.001$) cohorts. *Post hoc* analysis revealed significant differences in heat hyperalgesia between each heterozygous variant and its respective control (Fig. 2). In addition, male p−/m+ mice were found to be significantly more sensitive to heat stimulation than male p+/m− mice ($p<0.05$), while female p+/m− mice did not differ significantly from female p−/m+ mice (Fig. 2).

Acoustic startle

Statistically significant genotype differences in acoustic startle were observed amongst the female ($F_{2,161}=23.24$, $p<0.001$) and male ($F_{2,166}=14.78$, $p<0.001$) cohorts. In general, at

acoustic intensities of between 100–120 dB, heterozygotes (p+/m− and p−/m+) of both genders displayed lower startle responses in comparison to controls (Fig. 3).

Prepulse inhibition (PPI)

Significant genotype differences were found in regards to PPI of the acoustic startle reflex amongst female genotype variants ($F_{2,99}$=4.16, p<0.05) and amongst male genotype variants ($F_{2,96}$=14.22, p<0.001). However, Bonferroni *post hoc* tests found no significant differences between female heterozygotes and controls. At prepulse intensities of 70 dB and 80 dB *post hoc* analysis indicated a significant increase in PPI of male p−/m+ mice relative to controls, as well as a significant difference between p−/m+ and p+/m− male mice (Fig. 4).

Rotarod

Motor learning and sensorimotor coordination, as measured by the latency to fall off an accelerating rotarod, revealed significant genotype differences amongst female genotype variants ($F_{2,154}$=11.10, p<0.001) and male genotype variants ($F_{2,140}$=9.35, p<0.001). *Post hoc* analysis revealed significant differences between female p−/m+ and control mice on trial days 2, 3 and 7, while no significant difference was noted between female p+/m− mice and controls (Fig. 5). Mean weights ± SEM of female mice were: +/+ 23 ± 1, p+/m− 22 ± 1 and p−/m+ 26 ± 1 g. Male heterozygotes appeared to reach a plateau in their ability to improve their performance on the rotarod with *post hoc* analysis revealing significant differences between male heterozygotes of both variant (p+/m− and p−/m+) and male controls on days 5–7 (Fig. 5). Mean weights ± SEM of male mice were: +/+ 30 ± 2, p+/m− 30 ± 2 and p−/m+ 31 ± 1 g.

Marble burying

We observed no gender difference in the number of marbles buried by male or female control mice as has also been reported elsewhere [26, 46]. Significant genotype differences in marble burying behavior was observed amongst female mouse variants ($F_{2,41}$=4.86, p<0.05) with *post hoc* tests revealing female p−/m+ mice, but not p+/m− mice, to be significantly different from female controls (p<0.01). Likewise, a significant genotype difference in marble burying behavior was also observed between male mouse variants ($F_{2,41}$=4.26, p<0.05) with *post hoc* tests indicating male p−/m+ mice, but not male p+/m− mice, to be significantly different from male controls (p<0.05) (Table 1).

Wire hanging test

No significant gender difference in wire hanging behavior was observed between control mice (Table 2). In addition, no significant genotype difference in wire hanging performance was observed between female genotype variants ($F_{2,27}$=0.04, p=0.96) or male genotype variants ($F_{2,31}$=2.25, p=0.12) (Table 1). Weights and ages (mean ± SD) of mice used in the wire hanging task were: male, 26 ± 2 g, 12 ± 2 weeks old and female, 24 ± 3 g, 15 ± 4 weeks old.

PTZ seizure threshold

PTZ induced seizure scores for each genotype variant are presented in Table 1. Significant genotype differences were observed amongst females [H(3)=13.18, p<0.01] and male mouse variants [H(3)=14.89, p<0.001]. Within gender comparison revealed both female p+/m− and p−/m+ to be significantly more sensitive to the effects of PTZ than were female controls, p<0.01 and p<0.001, respectively, with no significant difference observed between female p+/m− and p−/m+ mice (Table 1). Within gender comparisons revealed both male p+/m− and p−/m+ to be significantly more sensitive to the effects of PTZ than were male controls

($p<0.001$ and $p<0.01$, respectively), with no significant difference observed between male p+/m− and p−/m+ mice.

Gene expression

Kruskal-Wallis analysis revealed significant group differences in *Gabrb3* expression between same gender genotypes in the DRG (female [H(3)=11.42, p<0.01]; male [H(3)=10.59, p<0.01]), spinal cord (female [H(3)=8.19, p<0.05]; male [H(3)=8.00, p<0.05]) and whole brain (female [H(3)=7.71, p<0.05]; male [H(3)=10.66, p<0.01]). Mann-Whitney *U post hoc* tests further indicated significant reductions of *Gabrb3* gene expression in heterozygous variants, compared to same-gender controls. However, no significant differences were observed between heterozygous variants of the same gender (Table 2).

The mRNA extracted from the RTN (Fig 6A) revealed significant group difference amongst the genotypes in regards to *Gabrb3* expression as indicated by the Kruskal-Wallis test (females: [H(3)=9.08, $p<0.05$]; males: [H(3)=14.64, $p<0.001$]). Mann-Whitney *U post hoc* tests indicated that all heterozygotes exhibited significantly less *Gabrb3* expression than gender-matched controls and that male p+/m− mice exhibited significantly less *Gabrb3* expression than male p−/m+ mice, whereas, no significant difference was detected between female heterozygotes (Fig. 6B). The maximum % variability in the housekeeping gene β-actin between same gender samples was 3%. Raw C_t values (mean ± SEM) were as follows: male, +/+ 31.1 ± 0.6; p−/m+ 32.7 ± 0.4; p+/m− 32.6 ± 0.4; Female, +/+ 30.4 ± 1.0; p−/m+ 32.1 ± 0.5, p+/m− 33.0 ± 0.3.

The mRNA extracted from the BNST (Fig. 7A) revealed significant group differences in regards to *Gabrb3* expression in males [H(3)=9.8, $p<0.01$], but not females [H(3)=5.52, $p>0.05$]. However, *post hoc* tests indicated that both male and female p−/m+ mice expressed significantly less *Gabrb3* than controls, $p<0.01$ and $p<0.05$, respectively while p+/m− mice did not (Fig. 7B). In addition, male p−/m+ mice expressed significantly less *Gabrb3* than male p+/m− mice ($p<0.01$) (Fig. 7B). The maximum % variability in β-actin between samples was 1% for the male samples and 4% for female samples. Raw C_t values (mean ± SEM) were as follows: male, +/+ 28.2 ± 1.6; p−/m+ 32.8 ± 0.7; p+/m− 32.3 ± 0.2; Female, +/+ 28.1 ± 1.2; p−/m+ 31.6 ± 0.4, p+/m− 32.2 ± 0.4.

The mRNA extracted from the amygdala (Fig. 8A) revealed significant group difference amongst genotypes, in regards to *Gabrb3* gene expression (females: [H(3)=11.00, $p<0.01$; males: [H(3)=9.76, $p<0.01$]). *Post hoc* tests indicated a significant reduction of *Gabrb3* expression in all heterozygotes relative to controls with no significant difference being observed between p+/m− and p−/m+ mice of the same gender (Fig. 8B). The maximum % variability in β-actin between samples was 4% for the male samples and 3% for female samples. Raw C_t values (mean ± SEM) were as follows: male, +/+ 31.9 ± 0.4; p−/m+ 31.9 ± 0.4; p+/m− 32.6 ± 0.6; Female, +/+ 30.4 ± 1.0; p−/m+ 31.7 ± 0.5, p+/m− 32.3 ± 0.2.

Discussion

All heterozygotes were overly sensitive to subthreshold heat stimuli, displayed reduced startle reactivity and were more susceptible to PTZ-induced seizures than gender-matched controls. Male heterozygotes also displayed tactile hypersensitivity and reduced sensorimotor competence on the accelerating rotarod, whereas female heterozygotes only exhibited mild effects in these two tasks. Furthermore, male p−/m+ mice were distinguishable from male p+/m− mice as having greater tactile and heat sensitivity as well as increased PPI. The presence of heightened seizure susceptibility, hypersensitivity to touch and heat and decreased sensorimotor competence are of particular interest as these features are common to ASD [6, 42, 57, 64].

Reductions in *Gabrb3* expression of between 46–59% were observed in whole brain, spinal cord and DRG of all heterozygous variants (Table 2). A previous study by Liljelund et. al. [38] involving *Gabrb3* heterozygotes maintained on a mixed background, reported an 80% decrease in β_3 protein content in whole brain, with the exception of male p−/m+ mice, which displayed a 37% reduction. These mice were described as being phenotypically normal with only subtle differences in EEG, however only a limited behavioral assessment was performed in that study. Both the current study and the Liljelund study indicate that a significant reductions in *Gabrb3* gene expression occurs in heterozygotes, likely causing an increase in excitability of the central nervous system, accounting for the observed EEG changes in the earlier study [38] and an increase in seizure susceptibility in the current study. A more in depth comparison between these two studies was not practical as the heterozygotes in the earlier study were of a mixed background and the assessments differed. Similar to the current study, the Liljelund study likewise concluded that differences observed between heterozygous mice was dependent on gender and parent-of-origin effects. Simple haploinsufficiency likely accounts for the seizure susceptibility in all heterozygotes in the current study, however, it does not provide much insight into why male heterozygotes were more affected than female heterozygotes in regards to sensorimotor competence and tactile sensitivity or why male p−/m+ mice were distinguishable from male p+/m− mice in regards to tactile and heat sensitivity as well as PPI.

Although, sensory processing involves numerous brain regions, virtually all sensory information passes through the thalamus, with thalamocortical neurons and their regulation by RTN neurons [27, 69] serving to filter the flow of information to the cortex. Two separate studies have implicated thalamic abnormalities in ASD, one involving proton spectroscopy of ASD brains [24] and the other suggesting that GABAergic dysfunction of the thalamus contributes to somatosensory-evoked response differences observed in Angelman syndrome, an ASD subtype, caused by a deletion of maternal chromosomal region 15q11-13, containing the *GABRB3* gene [14]. In addition, studies of *Gabrb3* knockout mice found highly abnormal RTN electrophysiology [31]. As GABAergic RTN neurons regulate the neuronal response of the ventral posterior medial thalamus to innocuous stimuli (light touch) [37] we chose to examine the RTN. *Gabrb3* expression in the RTN was significantly reduced in all heterozygous variants with male p+/m− mice exhibiting significantly less *Gabrb3* expression than their p−/m+ counterparts (Fig. 6B). Although intriguing, the expression data doesn't correlate well with the behavioral data, as one would have expected all heterozygotes to display significant differences in tactile sensitivity, with male p+/m− mice likely exhibiting the greatest degree of tactile hypersensitivity, which was not the case (Fig. 1). While the reduction in *Gabrb3* expression in the RTN likely contributes to the observed somatosensory hypersensitivity it doesn't provide a comprehensive understanding of why there are differences between heterozygous variants.

Reduced startle response was common to all heterozygotes, but only male p−/m+ mice displayed increase PPI. PPI serves as a model of sensorimotor gating [20], a process that serves to filter extraneous stimuli, thereby, protecting an organism from experiencing sensory overload, thus maintaining the integrity of higher cognitive processes [53]. Numerous midbrain structures mediate PPI [16, 62] with the BNST and the basolateral amygdala being indirectly linked to changes in PPI phenomena [58]. Similar reductions in *Gabrb3* expression in the amygdala were noted in all heterozygotes, thereby providing little insight into why male p−/m+ display significant increases in PPI and other heterozygous variants do not. However, the BNST in both female and male p−/m+ mice were found to express significantly less *Gabrb3* than controls, whereas, p+/m− of both genders oddly did not. The larger reduction in *Gabrb3* expression in the BNST of male p−/m+ mice versus female p−/m+ mice (72% vs. 43%) may be a contributing factor to the significant increase

in PPI observed in male p−/m+ mice but not female p−/m+ mice. Interestingly, the *Fmr1* knockout mouse, a model of Fragile × syndrome, a subtype of ASD, exhibits a reduction in acoustic startle reflex and an increase in PPI similar to male p−/m+ mice in this study [19]. The *Fmr1* knockout mouse also exhibits a down regulation in many elements of the GABA signaling system [8]. However, in contrast to these mouse models, individuals with Fragile × syndrome, idiopathic ASD or Asperger's syndrome exhibit a decrease in PPI [19, 40, 54]. Therefore, while the observation that both mouse models exhibit significant increases in PPI, supporting a role for these separate genes in sensorimotor gating, there is a lack of correspondence between the PPI phenotype observed in these mouse models and the human disorders they are suppose to represent [19, 40, 52, 54]. Therefore, while PPI circuitry in rodents can serve as a model for understanding the neural control of sensorimotor gating, presuming that the neural circuitry for PPI in rodents can necessarily be translated directly across species would be imprudent.

Marble burying behavior in mice is thought to model obsessive-compulsive [46] and repetitive/perseverant behavior [63]. Previous studies utilizing the *V1aR* gene knockout mouse [13] and the *Gabrb3* gene knockout mouse [26], both models of ASD, reported reductions in marble burying behavior. In the current study, male and female p−/m+ mice also displayed reduced marble burying behavior while their p+/m− counterparts did not (Table 1). The above findings appear to be counterintuitive as one would have predicted that an autism model would exhibit more preservative behavior, not less, leading to an increase in marbles buried. We considered whether tactile hypersensitivity or hypotonia, both observed in *Gabrb3* knockout mice [26, 65], might account for reduced digging in p−/m+ mice. However, no evidence for hypotonia, as assessed by the wire-hanging task, was observed in any heterozygote and no association between tactile hypersensitivity and the number of marble buried was apparent. A potential explanation for the above data comes from a study correlating decreased marble burying with increased 5-HT expression in the dorsal raphe nucleus [68]. Excitatory release of 5-HT within the dorsal raphe is mediated by the locus coeruleus (LC) [56], a region that expresses an abundance of *Gabrb3* [39] and has been postulated to be functionally impaired in ASD [41]. The LC has subsequently been found to be abnormal in *Gabrb3* knockout mice [26] thereby making it conceivable that decreased marble burying behavior exhibited by p−/m+ mice, as well as *Gabrb3* knockout mice [26], may indirectly entail changes in LC regulation of 5-HT function. Alternatively, electrode mapping studies have linked digging behavior with the distribution of hypothalamic efferent fibers from the BNST [36]. Therefore, a potential scenario might include a significant reduction in *Gabrb3* expression in BNST resulting in reduced burying/digging behavior as seen in p−/m+ mice. The BNST is most often associated with stress-responsiveness and emotionality [43], but is also involved in the expression of maternal and paternal behavior (for review, see [47]). Therefore, rather than perseverant behavior, the reduction in marble burying (i.e. reduced digging behavior) observed in this study, may be indicative of a change in a parental social behavior, such as nest building, which involves digging behavior [22, 70]. Moreover, deficits in nesting and digging behavior as well as abnormal social behavior have been previously observed in *Gabrb3* knockout mice [12]. As abnormal social behavior is a hallmark of ASD, an in-depth evaluation of social behavior in these heterozygotes is warranted.

The current findings indicate that simple haploinsufficiency due to heterozygous disruption of the *Gabrb3* gene, on a relatively homogenous C57BL/6J background, is sufficient to manifest behaviors often present in ASD. These include heightened heat sensitivity and increased seizure susceptibility. However, differences between heterozygous variants in tactile sensitivity, heat sensitivity and PPI along with concurrent differences in *Gabrb3* expression in the RTN and BNST suggest other mechanisms besides haploinsufficiency are involved. The observation that male heterozygotes were more robustly affected in regards to

tactile sensitivity and sensorimotor competence than were female heterozygotes is of particular interest as ASD exhibits a strong male bias. These results suggest the *Gabrb3* gene may exhibit gender dependent regulation allowing phenotypic manifestation to be more apparent in males [18]. In addition, both *Gabrb3* expression and behavior appear to be significantly influenced by whether the intact *Gabrb3* gene contributed to the heterozygous offspring is of paternal or maternal origin. Although the *GABRB3* gene is not imprinted and expresses biallelically in normal human and mouse brain [5, 28, 45], in situations where only one chromosomal allele containing the *GABRB3* gene is present, a paternal expression bias of the *GABRB3* gene has been indicated [2, 3, 28, 35]. Hogart et. al., [28] hypothesized that a complex epigenetic dysregulation of the chromosomal region containing the *GABRB3* gene occurs in situations where only one chromosomal allele is present with the paternal allele likely containing a more active chromatin configuration than the maternal allele. A parental expression bias was noted in our mouse model in regards to *Gabrb3* expression in the the BNST as well as in the behavioral data, suggesting that a paternal deletion of the *Gabrb3* gene leads to a more robust behavioral phenotype. Lastly, the presence of tactile and heat hypersensitivity in these mice, both common to ASD, is an important finding, as these behaviors have not been previously observed in other ASD mouse models. Understanding the source of such sensory hypersensitivities is paramount to the development of intervention strategies aimed at maximizing the coping ability of autistic individuals whose lives are strongly impacted by sensory over-stimulation. The current findings are congruent with the wealth of evidence implicating the *GABRB3* gene in ASD and lend strong support for utilizing this mouse model to further investigate other behavioral abnormalities typical of ASD.

Acknowledgments

This work was supported by NIMH grant RO1MH65393 to Timothy M. DeLorey.

References

1. Abrahams BS, Geschwind DH. Advances in autism genetics: on the threshold of a new neurobiology. Nat Rev Genet. 2008; 9:341–55. [PubMed: 18414403]
2. Bittel DC, Kibiryeva N, Talebizadeh Z, Butler MG. Microarray analysis of gene/transcript expression in Prader-Willi syndrome: deletion versus UPD. J Med Genet. 2003; 40:568–74. [PubMed: 12920063]
3. Bittel DC, Kibiryeva N, Talebizadeh Z, Driscoll DJ, Butler MG. Microarray analysis of gene/transcript expression in Angelman syndrome: deletion versus UPD. Genomics. 2005; 85:85–91. [PubMed: 15607424]
4. Bonnert TP, McKernan RM, Farrar S, le Bourdelles B, Heavens RP, Smith DW, et al. theta, a novel gamma-aminobutyric acid type A receptor subunit. Proc Natl Acad Sci U S A. 1999; 96:9891–6. [PubMed: 10449790]
5. Buettner VL, Longmate JA, Barish ME, Mann JR, Singer-Sam J. Analysis of imprinting in mice with uniparental duplication of proximal chromosomes 7 and 15 by use of a custom oligonucleotide microarray. Mamm Genome. 2004; 15:199–209. [PubMed: 15014969]
6. Cascio C, McGlone F, Folger S, Tannan V, Baranek G, Pelphrey KA, et al. Tactile perception in adults with autism: a multidimensional psychophysical study. J Autism Dev Disord. 2008; 38:127–37. [PubMed: 17415630]
7. Chaplan SR, Bach FW, Pogrel JW, Chung JM, Yaksh TL. Quantitative assessment of tactile allodynia in the rat paw. J Neurosci Methods. 1994; 53:55–63. [PubMed: 7990513]
8. D'Hulst C, Heulens I, Brouwer JR, Willemsen R, De Geest N, Reeve SP, et al. Expression of the GABAergic system in animal models for fragile × syndrome and fragile × associated tremor/ataxia syndrome (FXTAS). Brain Res. 2009; 1253:176–83. [PubMed: 19070606]

9. Delahanty RJ, Kang JQ, Brune CW, Kistner EO, Courchesne E, Cox NJ, et al. Maternal transmission of a rare GABRB3 signal peptide variant is associated with autism. Mol Psychiatry. 2009
10. DeLorey, TM. GABRB3 Gene Deficient Mice: A Potential Model of Autism Spectrum Disorder. In: Dhossche, D., editor. GABA in Autism and Related Disorders. Vol. 71. New York: Elsevier Science Publishing Co., Inc; 2005. p. 259-382.
11. DeLorey TM, Handforth A, Anagnostaras SG, Homanics GE, Minassian BA, Asatourian A, et al. Mice lacking the beta3 subunit of the GABAA receptor have the epilepsy phenotype and many of the behavioral characteristics of Angelman syndrome. J Neurosci. 1998; 18:8505–14. [PubMed: 9763493]
12. DeLorey TM, Sahbaie P, Hashemi E, Homanics GE, Clark JD. Gabrb3 gene deficient mice exhibit impaired social and exploratory behaviors, deficits in non-selective attention and hypoplasia of cerebellar vermal lobules: A potential model of autism spectrum disorder. Behav Brain Res. 2008; 187:207–20. [PubMed: 17983671]
13. Egashira N, Tanoue A, Matsuda T, Koushi E, Harada S, Takano Y, et al. Impaired social interaction and reduced anxiety-related behavior in vasopressin V1a receptor knockout mice. Behav Brain Res. 2007; 178:123–7. [PubMed: 17227684]
14. Egawa K, Asahina N, Shiraishi H, Kamada K, Takeuchi F, Nakane S, et al. Aberrant somatosensory-evoked responses imply GABAergic dysfunction in Angelman syndrome. Neuroimage. 2008; 39:593–9. [PubMed: 17962046]
15. Fatemi SH, Reutiman TJ, Folsom TD, Thuras PD. GABA(A) Receptor Downregulation in Brains of Subjects with Autism. J Autism Dev Disord. 2009; 39:223–30. [PubMed: 18821008]
16. Fendt M, Li L, Yeomans JS. Brain stem circuits mediating prepulse inhibition of the startle reflex. Psychopharmacology (Berl). 2001; 156:216–24. [PubMed: 11549224]
17. Field MJ, Bramwell S, Hughes J, Singh L. Detection of static and dynamic components of mechanical allodynia in rat models of neuropathic pain: are they signalled by distinct primary sensory neurones? Pain. 1999; 83:303–11. [PubMed: 10534603]
18. Fombonne E. The epidemiology of autism: a review. Psychol Med. 1999; 29:769–86. [PubMed: 10473304]
19. Frankland PW, Wang Y, Rosner B, Shimizu T, Balleine BW, Dykens EM, et al. Sensorimotor gating abnormalities in young males with fragile × syndrome and Fmr1-knockout mice. Mol Psychiatry. 2004; 9:417–25. [PubMed: 14981523]
20. Geyer MA, McIlwain KL, Paylor R. Mouse genetic models for prepulse inhibition: an early review. Mol Psychiatry. 2002; 7:1039–53. [PubMed: 12476318]
21. Gillberg C, Nordin V, Ehlers S. Early detection of autism. Diagnostic instruments for clinicians. Eur Child Adolesc Psychiatry. 1996; 5:67–74. [PubMed: 8814412]
22. Gonzalez-Mariscal G, Chirino R, Rosenblatt JS, Beyer C. Forebrain implants of estradiol stimulate maternal nest-building in ovariectomized rabbits. Horm Behav. 2005; 47:272–9. [PubMed: 15708755]
23. Greenspan S, Weider S. Developmental patterns and outcomes in infants and children with disorders in relating and communicating: a chart review of 200 cases of children with autistic spectrum diagnosis. J Dev Learn Disord. 1997; 1:87–141.
24. Hardan AY, Minshew NJ, Melhem NM, Srihari S, Jo B, Bansal R, et al. An MRI and proton spectroscopy study of the thalamus in children with autism. Psychiatry Res. 2008; 163:97–105. [PubMed: 18508243]
25. Hargreaves K, Dubner R, Brown F, Flores C, Joris J. A new and sensitive method for measuring thermal nociception in cutaneous hyperalgesia. Pain. 1988; 32:77–88. [PubMed: 3340425]
26. Hashemi E, Sahbaie P, Davies MF, Clark JD, Delorey TM. Gabrb3 gene deficient mice exhibit increased risk assessment behavior, hypotonia and expansion of the plexus of locus coeruleus dendrites. Brain Res. 2007; 1129:191–9. [PubMed: 17156762]
27. Hirata A, Aguilar J, Castro-Alamancos MA. Noradrenergic activation amplifies bottom-up and top-down signal-to-noise ratios in sensory thalamus. J Neurosci. 2006; 26:4426–36. [PubMed: 16624962]

28. Hogart A, Nagarajan RP, Patzel KA, Yasui DH, Lasalle JM. 15q11-13 GABAA receptor genes are normally biallelically expressed in brain yet are subject to epigenetic dysregulation in autism-spectrum disorders. Hum Mol Genet. 2007; 16:691–703. [PubMed: 17339270]
29. Homanics GE, DeLorey TM, Firestone LL, Quinlan JJ, Handforth A, Harrison NL, et al. Mice devoid of gamma-aminobutyrate type A receptor beta3 subunit have epilepsy, cleft palate, and hypersensitive behavior. Proc Natl Acad Sci U S A. 1997; 94:4143–8. [PubMed: 9108119]
30. Homanics GE, Quinlan JJ, Firestone LL. Pharmacologic and behavioral responses of inbred C57BL/6J and strain 129/SvJ mouse lines. Pharmacol Biochem Behav. 1999; 63:21–6. [PubMed: 10340519]
31. Huntsman MM, Porcello DM, Homanics GE, DeLorey TM, Huguenard JR. Reciprocal inhibitory connections and network synchrony in the mammalian thalamus. Science. 1999; 283:541–3. [PubMed: 9915702]
32. Insel TR. Mouse models for autism: report from a meeting. Mamm Genome. 2001; 12:755–7. [PubMed: 11678137]
33. Kern JK, Trivedi MH, Garver CR, Grannemann BD, Andrews AA, Savla JS, et al. The pattern of sensory processing abnormalities in autism. Autism. 2006; 10:480–94. [PubMed: 16940314]
34. Kogan MD, Blumberg SJ, Schieve LA, Boyle CA, Perrin JM, Ghandour RM, et al. Prevalence of Parent-Reported Diagnosis of Autism Spectrum Disorder Among Children in the US, 2007. Pediatrics. 2009; 124:1395–403. [PubMed: 19805460]
35. Kubota T, Niikawa N, Jinno Y, Ishimaru T. GABAA receptor beta 3 subunit gene is possibly paternally imprinted in humans. Am J Med Genet. 1994; 49:452–3. [PubMed: 8160743]
36. Lammers JH, Meelis W, Kruk MR, van der Poel AM. Hypothalamic substrates for brain stimulation-induced grooming, digging and circling in the rat. Brain Res. 1987; 418:1–19. [PubMed: 3664265]
37. Lee SM, Friedberg MH, Ebner FF. The role of GABA-mediated inhibition in the rat ventral posterior medial thalamus. I. Assessment of receptive field changes following thalamic reticular nucleus lesions. J Neurophysiol. 1994; 71:1702–15. [PubMed: 8064343]
38. Liljelund P, Handforth A, Homanics GE, Olsen RW. GABAA receptor beta3 subunit gene-deficient heterozygous mice show parent-of-origin and gender-related differences in beta3 subunit levels, EEG, and behavior. Brain Res Dev Brain Res. 2005; 157:150–61.
39. Luque JM, Malherbe P, Richards JG. Localization of GABAA receptor subunit mRNAs in the rat locus coeruleus. Brain Res Mol Brain Res. 1994; 24:219–26. [PubMed: 7968361]
40. McAlonan GM, Daly E, Kumari V, Critchley HD, van Amelsvoort T, Suckling J, et al. Brain anatomy and sensorimotor gating in Asperger's syndrome. Brain. 2002; 125:1594–606. [PubMed: 12077008]
41. Mehler MF, Purpura DP. Autism, fever, epigenetics and the locus coeruleus. Brain Res Rev. 2009; 59:388–92. [PubMed: 19059284]
42. Ming X, Brimacombe M, Wagner GC. Prevalence of motor impairment in autism spectrum disorders. Brain Dev. 2007; 29:565–70. [PubMed: 17467940]
43. Morilak DA, Barrera G, Echevarria DJ, Garcia AS, Hernandez A, Ma S, et al. Role of brain norepinephrine in the behavioral response to stress. Prog Neuropsychopharmacol Biol Psychiatry. 2005; 29:1214–24. [PubMed: 16226365]
44. Moy SS, Nadler JJ, Young NB, Perez A, Holloway LP, Barbaro RP, et al. Mouse behavioral tasks relevant to autism: phenotypes of 10 inbred strains. Behav Brain Res. 2007; 176:4–20. [PubMed: 16971002]
45. Nicholls RD, Gottlieb W, Russell LB, Davda M, Horsthemke B, Rinchik EM. Evaluation of potential models for imprinted and nonimprinted components of human chromosome 15q11-q13 syndromes by fine-structure homology mapping in the mouse. Proc Natl Acad Sci U S A. 1993; 90:2050–4. [PubMed: 8095339]
46. Njung'e K, Handley SL. Evaluation of marble-burying behavior as a model of anxiety. Pharmacol Biochem Behav. 1991; 38:63–7. [PubMed: 2017455]
47. Numan, M.; Insel, T. The Neurobiology of Parental Behavior. New York: Springer; 2003.
48. Ochoa JL, Yarnitsky D. Mechanical hyperalgesias in neuropathic pain patients: dynamic and static subtypes. Ann Neurol. 1993; 33:465–72. [PubMed: 8388678]

49. Ogura H, Aruga J, Mikoshiba K. Behavioral abnormalities of Zic1 and Zic2 mutant mice: implications as models for human neurological disorders. Behav Genet. 2001; 31:317–24. [PubMed: 11699604]
50. Olsen, RW.; DeLorey, TM. GABA and Glycine. In: Siegel, GJ.; Agranoff, BW.; Albers, RW.; Fisher, SK.; Uhler, MD., editors. Basic Neurochemistry. New York: Lippincott-Raven; 1999. p. 335-346.
51. Paxinos, G.; Franklin, K. The Mouse Brain: In stereotaxic coordinates. San Diego: Academic Press; 2001. p. 350
52. Paylor R, Yuva-Paylor LA, Nelson DL, Spencer CM. Reversal of sensorimotor gating abnormalities in Fmr1 knockout mice carrying a human Fmr1 transgene. Behav Neurosci. 2008; 122:1371–7. [PubMed: 19045956]
53. Perry W, Braff DL. Information-processing deficits and thought disorder in schizophrenia. Am J Psychiatry. 1994; 151:363–7. [PubMed: 8109644]
54. Perry W, Minassian A, Lopez B, Maron L, Lincoln A. Sensorimotor gating deficits in adults with autism. Biol Psychiatry. 2007; 61:482–6. [PubMed: 16460695]
55. Poree LR, Guo TZ, Kingery WS, Maze M. The analgesic potency of dexmedetomidine is enhanced after nerve injury: a possible role for peripheral alpha2-adrenoceptors. Anesth Analg. 1998; 87:941–8. [PubMed: 9768799]
56. Pudovkina OL, Cremers TI, Westerink BH. The interaction between the locus coeruleus and dorsal raphe nucleus studied with dual-probe microdialysis. Eur J Pharmacol. 2002; 445:37–42. [PubMed: 12065192]
57. Rapin I, Katzman R. Neurobiology of autism. Ann Neurol. 1998; 43:7–14. [PubMed: 9450763]
58. Risterucci C, Jeanneau K, Schoppenthau S, Bielser T, Kunnecke B, von Kienlin M, et al. Functional magnetic resonance imaging reveals similar brain activity changes in two different animal models of schizophrenia. Psychopharmacology (Berl). 2005; 180:724–34. [PubMed: 15726331]
59. Samaco RC, Hogart A, LaSalle JM. Epigenetic overlap in autism-spectrum neurodevelopmental disorders: MECP2 deficiency causes reduced expression of UBE3A and GABRB3. Hum Mol Genet. 2005; 14:483–92. [PubMed: 15615769]
60. Schwaller B, Tetko IV, Tandon P, Silveira DC, Vreugdenhil M, Henzi T, et al. Parvalbumin deficiency affects network properties resulting in increased susceptibility to epileptic seizures. Mol Cell Neurosci. 2004; 25:650–63. [PubMed: 15080894]
61. Shao Y, Cuccaro ML, Hauser ER, Raiford KL, Menold MM, Wolpert CM, et al. Fine mapping of autistic disorder to chromosome 15q11-q13 by use of phenotypic subtypes. Am J Hum Genet. 2003; 72:539–48. [PubMed: 12567325]
62. Swerdlow NR, Geyer MA, Braff DL. Neural circuit regulation of prepulse inhibition of startle in the rat: current knowledge and future challenges. Psychopharmacology (Berl). 2001; 156:194–215. [PubMed: 11549223]
63. Thomas A, Burant A, Bui N, Graham D, Yuva-Paylor LA, Paylor R. Marble burying reflects a repetitive and perseverative behavior more than novelty-induced anxiety. Psychopharmacology (Berl). 2009; 204:361–73. [PubMed: 19189082]
64. Tomchek SD, Dunn W. Sensory processing in children with and without autism: a comparative study using the short sensory profile. Am J Occup Ther. 2007; 61:190–200. [PubMed: 17436841]
65. Ugarte SD, Homanics GE, Firestone LL, Hammond DL. Sensory thresholds and the antinociceptive effects of GABA receptor agonists in mice lacking the beta3 subunit of the GABA(A) receptor. Neuroscience. 2000; 95:795–806. [PubMed: 10670447]
66. Wang H, Owens JD, Shih JH, Li MC, Bonner RF, Mushinski JF. Histological staining methods preparatory to laser capture microdissection significantly affect the integrity of the cellular RNA. BMC Genomics. 2006; 7:97. [PubMed: 16643667]
67. Witkin JM. Animal models of obsessive-compulsive disorder. Curr Protoc Neurosci. 2008; Chapter 9(Unit 9):30. [PubMed: 18972380]
68. Yamada K, Wada E, Yamano M, Sun YJ, Ohara-Imaizumi M, Nagamatsu S, et al. Decreased marble burying behavior in female mice lacking neuromedin-B receptor (NMB-R) implies the

involvement of NMB/NMB-R in 5-HT neuron function. Brain Res. 2002; 942:71–8. [PubMed: 12031854]

69. Yen CT, Shaw FZ. Reticular thalamic responses to nociceptive inputs in anesthetized rats. Brain Res. 2003; 968:179–91. [PubMed: 12663087]
70. Yunes RM, Cutrera RA, Castro-Vazquez A. Nesting and digging behavior in three species of Calomys (Rodentia; Cricetidae). Physiol Behav. 1991; 49:489–92. [PubMed: 2062924]

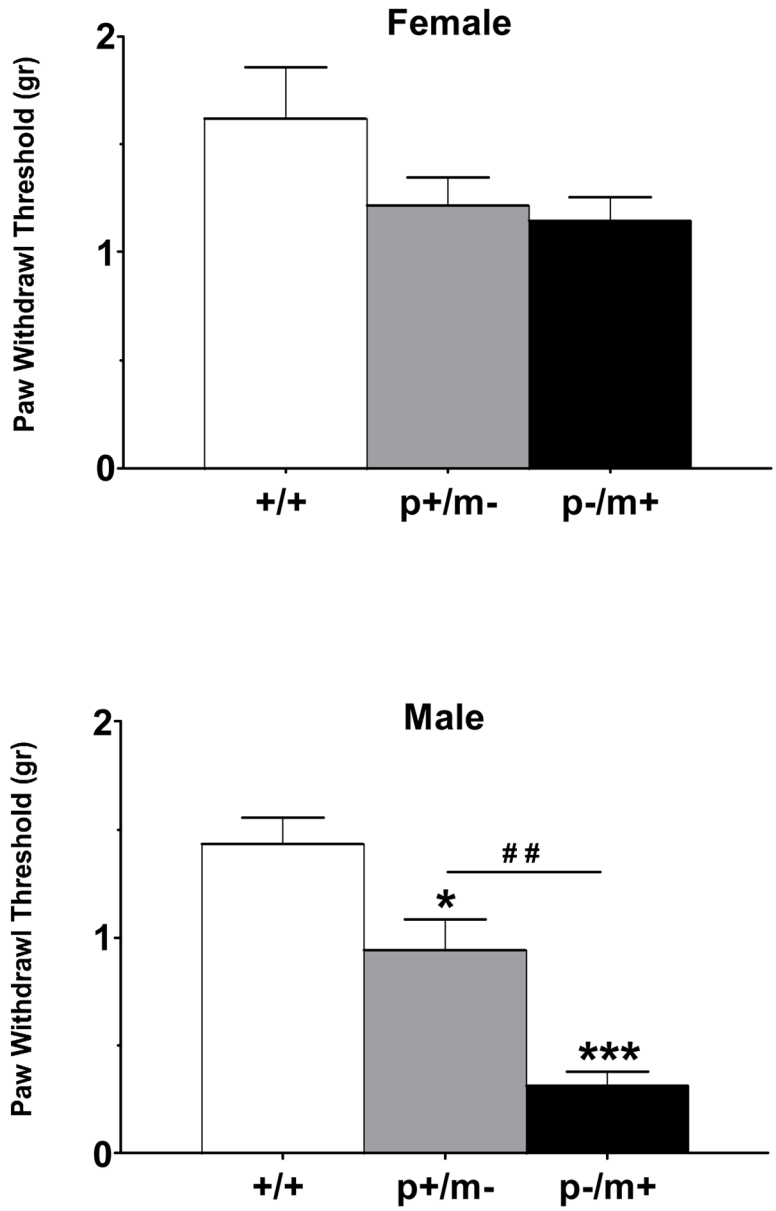

Figure 1.

Histograms depicting paw withdrawal thresholds (mean ± SEM) elicited by applying von Frey monofilaments to the planter surface of the hindpaw. Mice of both genders harboring the disrupted *Gabrb3* gene on either the maternal (p+/m−) or paternal (p−/m+) chromosomal allele were tested for mechanical sensitivity. Female +/+, n=14; female p+/m−, n=16; female p−/m+, n=18. Male +/+, n=15; male p+/m−, n=14; male p−/m+, n=14. *p<0.05, ***p<0.001 represents difference from gender-matched controls; ##p<0.01 represents difference between male p+/m− and p−/m+ mice.

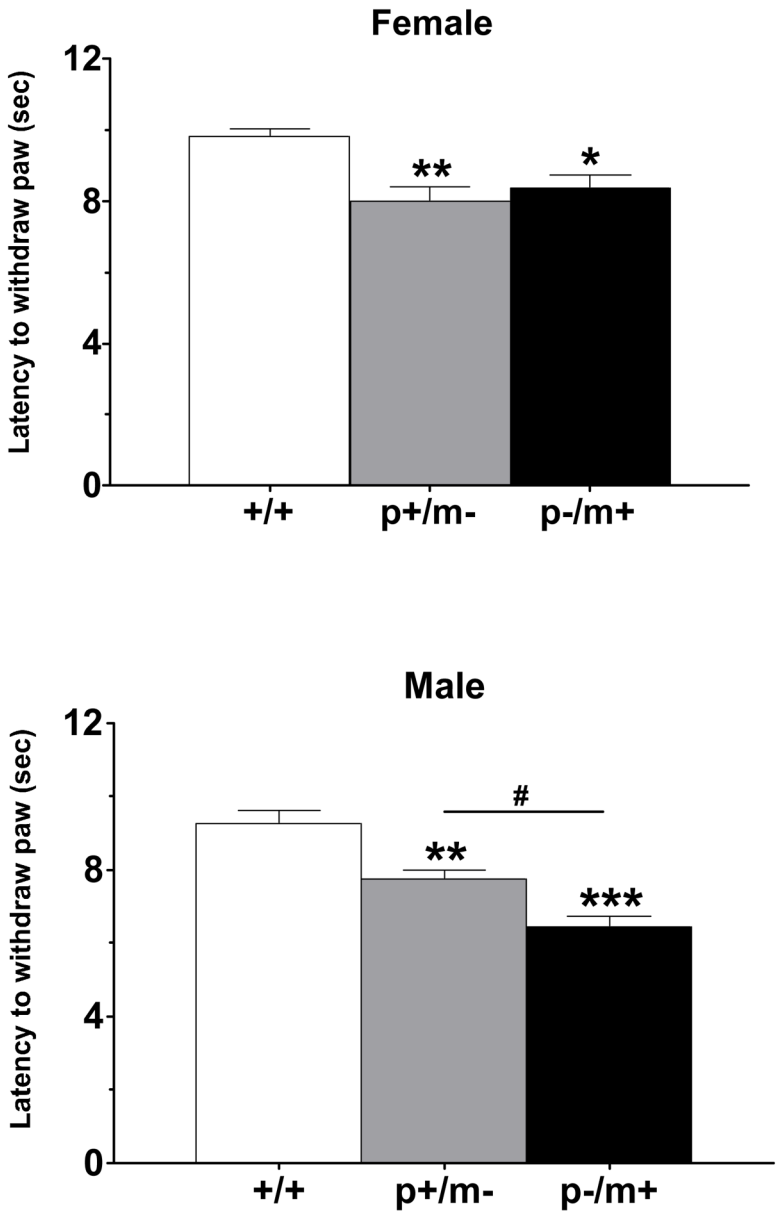

Figure 2.

Histograms depicting paw withdrawal latencies (mean ± SEM) to radiant heat, as measured by the Hargreaves method. Each genotype group consisted of seven mice. *p<0.05, **p<0.01, ***p<0.001 indicates significant differences from gender-matched controls, #p<0.05 represents difference between p+/m− and p−/m+ male mice.

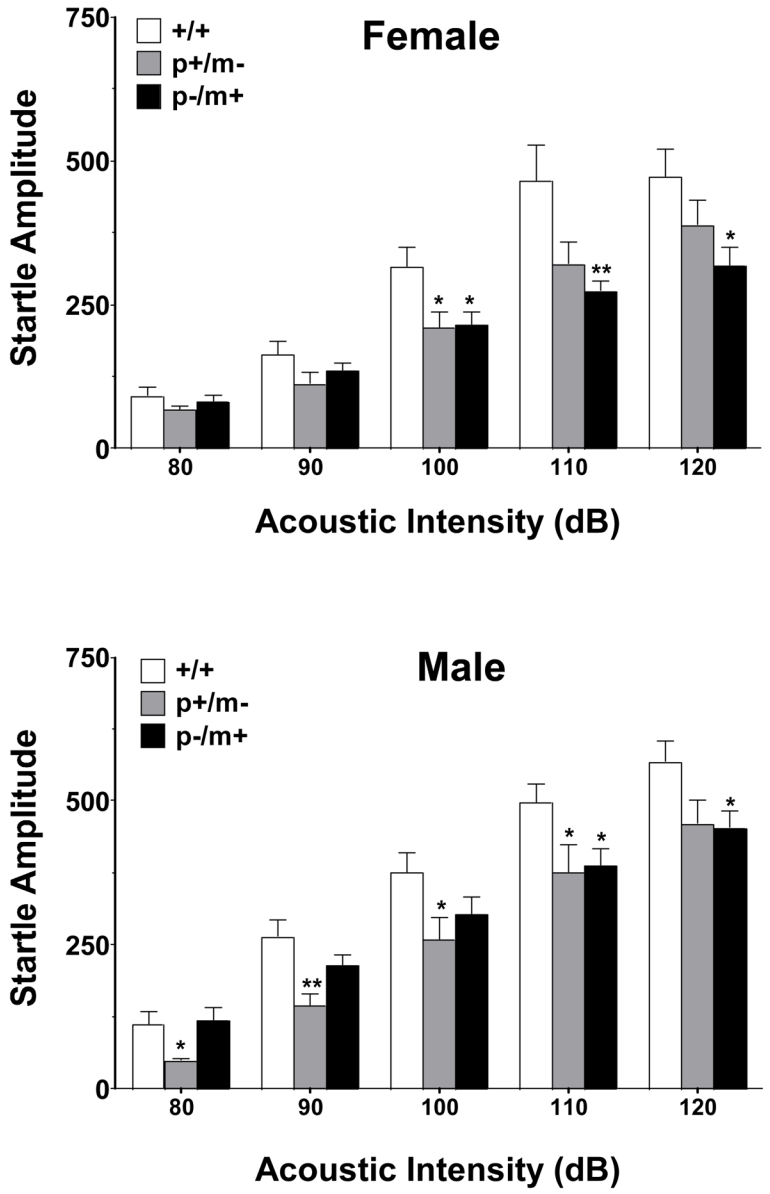

Figure 3.

Acoustic startle threshold responsivity of heterozygous and control mice. Histograms depict the mean peak response amplitude ± SEM of 10 trials using five separate startle stimuli ranging from 80–120 dB. Female mice: +/+, n=12; p+/m−, n=12; p−/m+, n=12. Male mice: +/+, n=13; p+/m−, n=11; p−/m+, n=13. *p<0.05, **p<0.01 indicates significant differences from gender-matched controls.

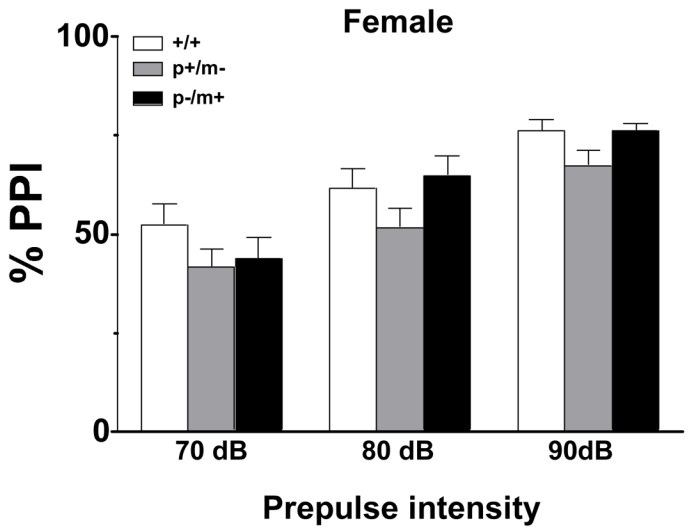

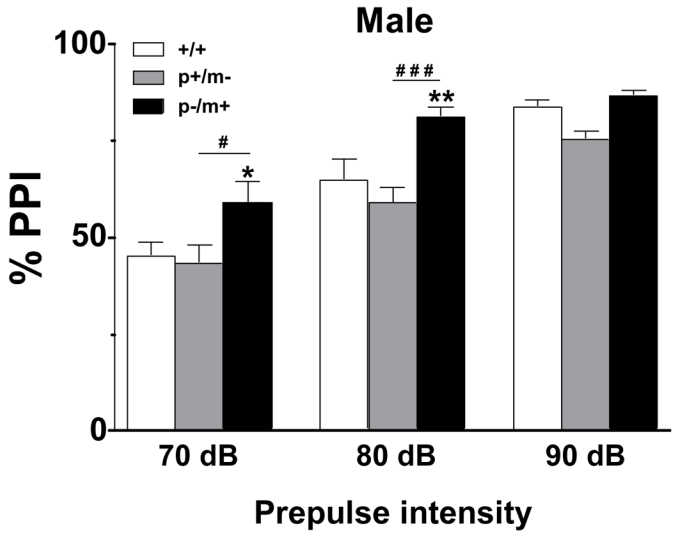

Figure 4.

Assessment of prepulse inhibition (PPI) in heterozygous and control mice. PPI was examined using prepulses of different intensities, 70, 80 and 90 dB, and presented as percentages (mean ± SEM) using the formula: % PPI= 100 − [(startle response with prepulse presented before the startle stimulus/startle stimulus response alone) × 100]. A high % prepulse inhibition value indicates that the subject showed a reduced startle response when a prepulse stimulus was presented compared to when the startle stimulus was presented alone. Female mice: +/+, n=12; p+/m−, n=12; p−/m+, n=12. Male mice: +/+, n=13; p+/m−, n=11; p−/m+, n=13. *p<0.05, **p<0.01 indicates significant difference from gender-matched controls, #p<0.05, ###p<0.001 represents difference between p+/m− and p −/m+ male mice.

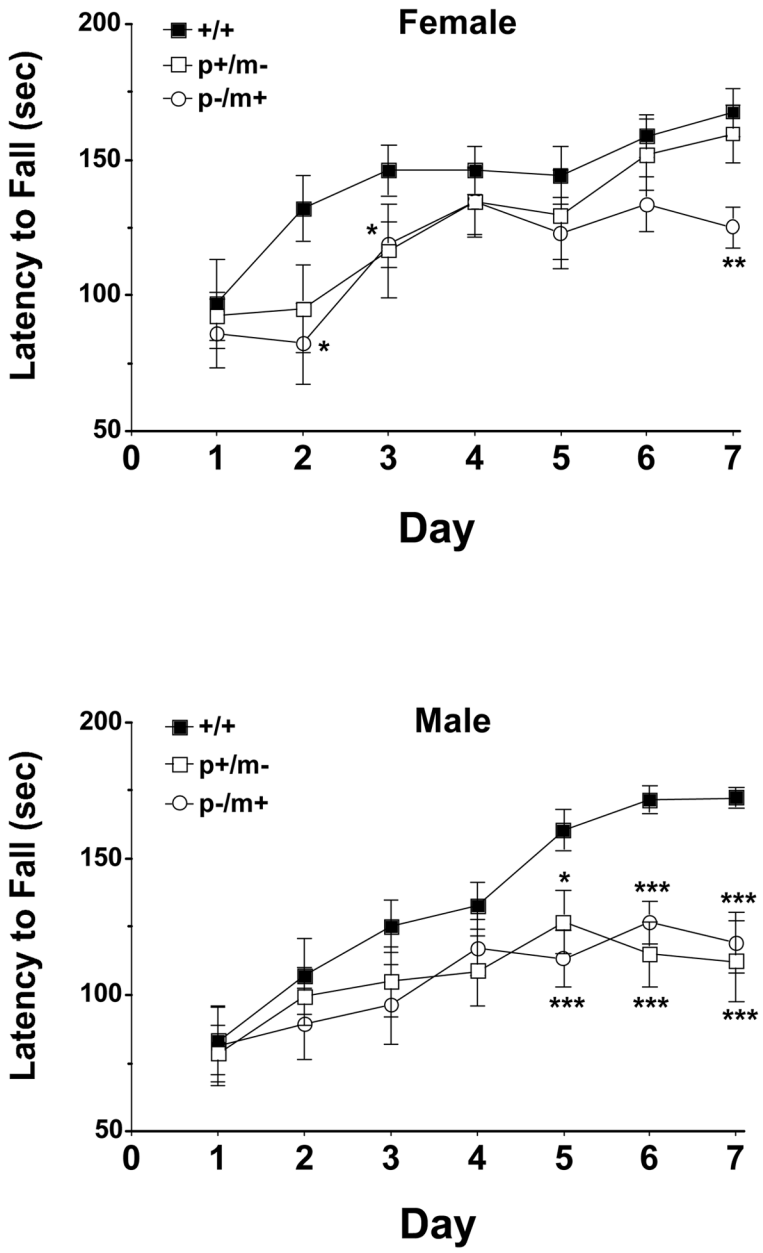

Figure 5.

Assessment of the performance of heterozygous and control mice on the accelerating rotarod. Mice were placed on a stationary rod for 30 sec prior to slowly rotating the rod from 3 to 19 rpm over a 180 sec trial period, performed once a day for 7 consecutive days. Data are presented as the mean ± SEM of the time in which each mouse genotype was able to remain on the rod. Female mice n=12 for each genotype, male mice n=11 for each genotype. Significant differences relative to gender-matched control mice are as indicated *$p<0.05$, **$p<0.01$, ***$p<0.001$.

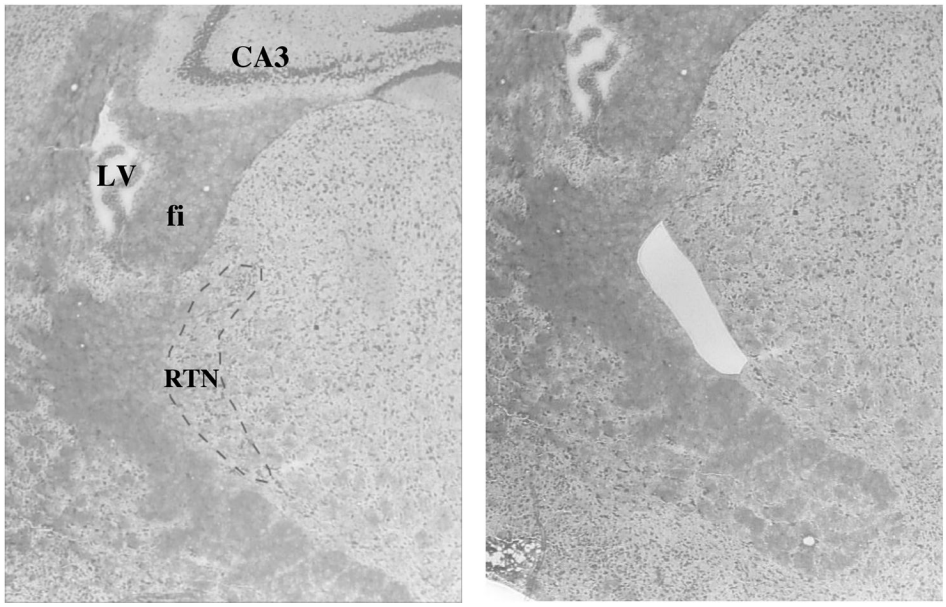

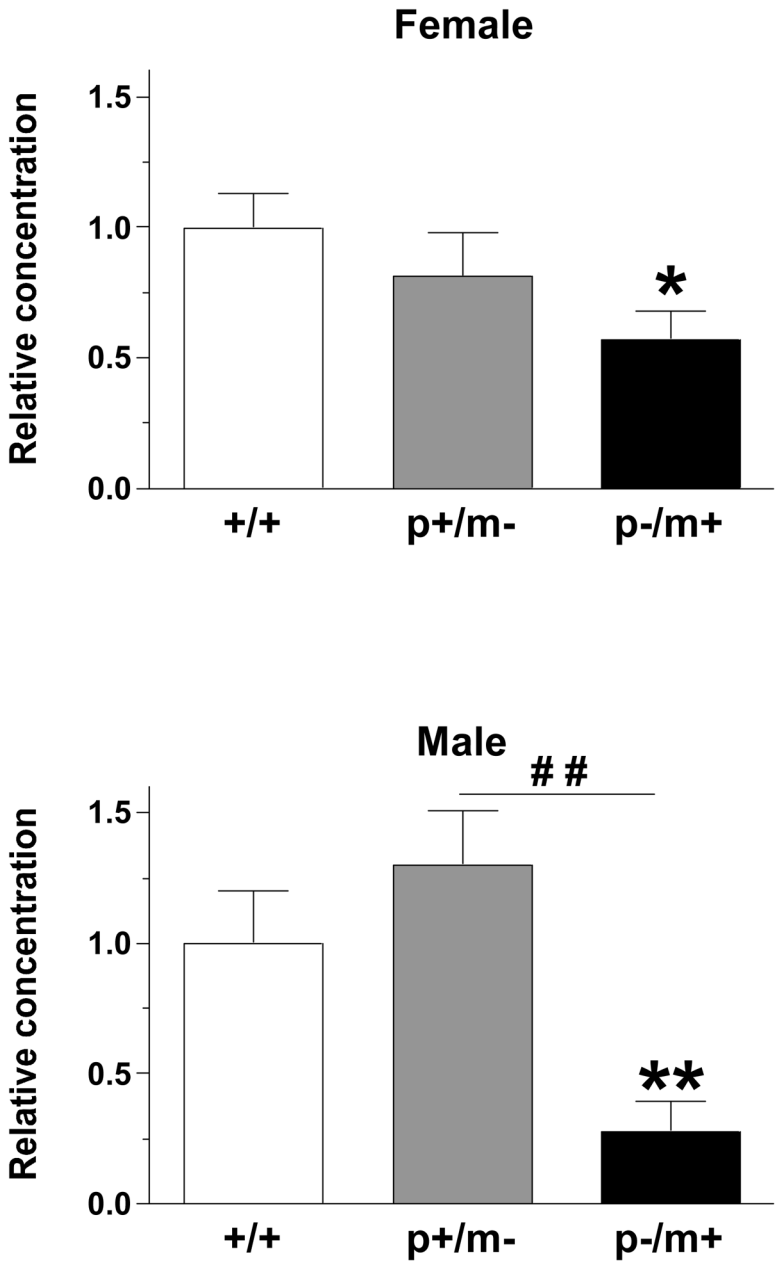

Figure 6.

A) Representative example of the region of the reticular thalamic nucleus (RTN) (bregma −1.46, 4X magnification, outlined by the dashed line) that was removed by laser capture microdissection. For reference the lateral ventricle (LV), fimbria of the hippocampus (fi), and the CA3 field of the hippocampus have been labeled. **B)** Histograms depicting the expression levels of *Gabrb3* (mean ± SEM) in the RTN, relative to expression in gender-matched controls (n=5–7 per genotype). *p<0.05, **p<0.01 represents significant difference from controls, whereas ##p<0.01 represents significant differences between male p+/m− and p−/m+ mice.

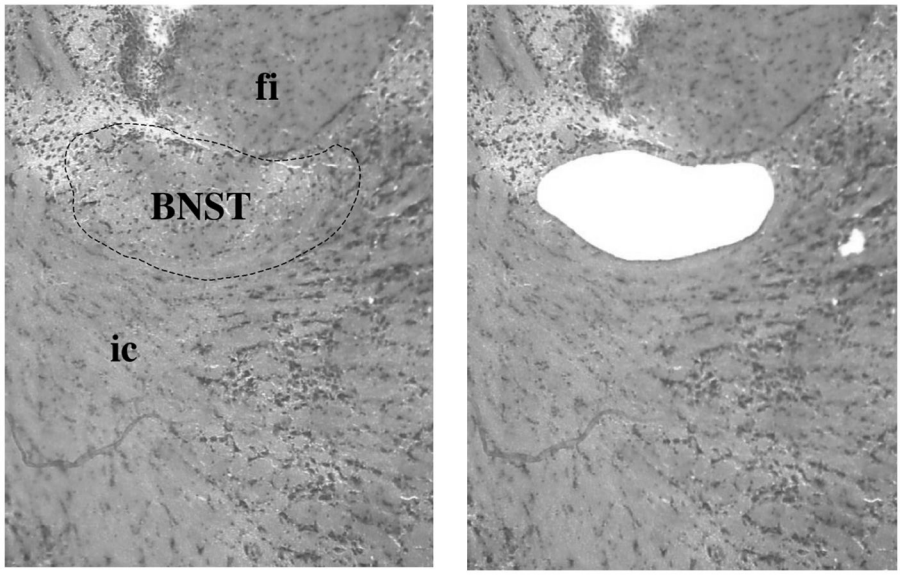

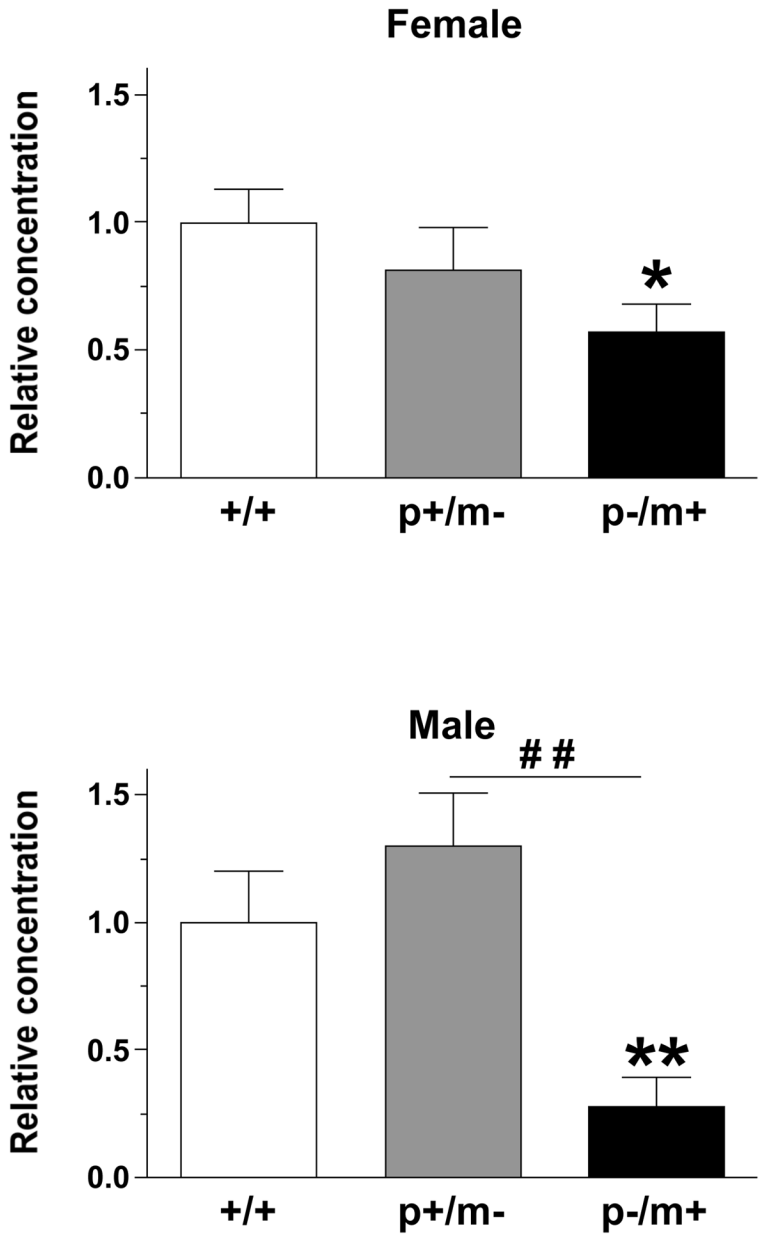

Figure 7.

A) Representative example of the bed nucleus of the stria terminalis, supracapsular part (BNST) (bregma −1.22, 10X magnification, outlined by dashed line) that was removed by laser capture microdissection. For reference the fimbria of the hippocampus (fi) and the internal capsule (ic) have been labeled. **B)** Histograms depicting the expression level of *Gabrb3* (mean ± SEM) in the BNST, relative to expression in gender-matched controls (n=5–7 per genotype). **p*<0.05, ***p*<0.01 indicates significant differences from controls, whereas ##*p*<0.01 represents significant differences between male p+/m− and p−/m+ mice.

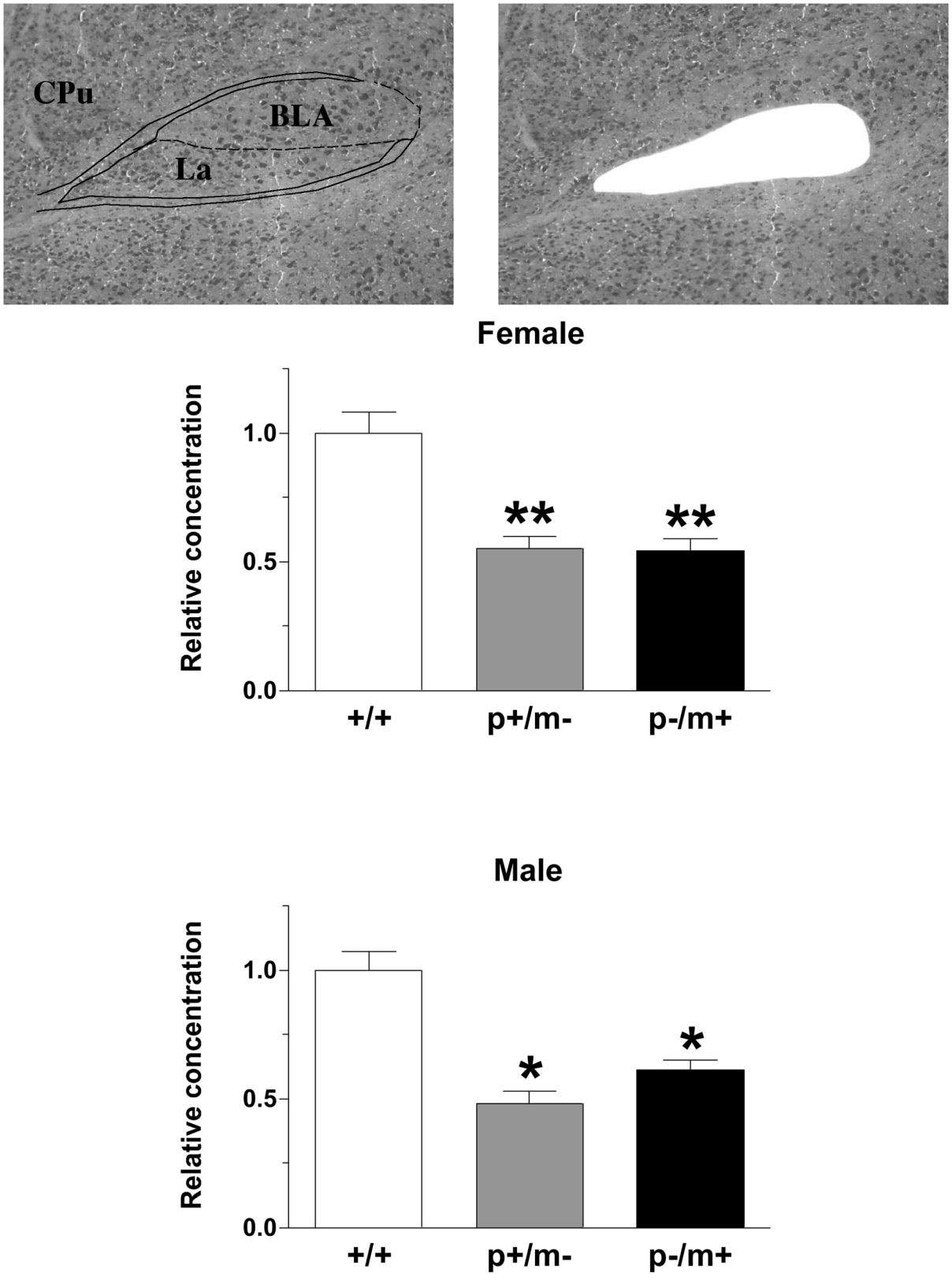

Figure 8.

A) Representative example of the amygdala including the basolateral amygdaloid nucleus, anterior part (BLA) and the lateral amygdaloid nucleus (LA) (bregma −1.06, 10X magnification, outlined by the solid lines) that was removed by laser capture microdissection. For reference the caudate putamen (CPu) has been labeled. **B)** Histograms depicting the expression of *Gabrb3* (mean ± SEM) in the amygdala, relative to expression in gender-matched controls (n=4–6 per genotype). **p*<0.05, ***p*<0.01 represents significant differences relative to controls.

Table 1

Behavioral analysis of heterozygous mice compared to controls.

Genotype	Marble burying[a]	Wire hanging[b]	Seizure susceptibility[c]
Female			
+/+	17 ± 1	29.3 ± 4.6	1.9 ± 0.3
p+/m−	15 ± 2	30.5 ± 4.8	5.4 ± 1.0**
p−/m+	11 ± 2**	31.2 ± 5.5	6.8 ± 1.4**
Male			
+/+	19 ± 1	22.0 ± 3.8	1.5 ± 0.3
p+/m−	17 ± 1	27.4 ± 4.4	5.3 ± 0.8***
p−/m+	14 ± 2*	35.8 ± 5.4	5.2 ± 1.2**

Data presented as the mean ± SEM.

[a] Number of marbles buried during a 30 min period, n=12–18.

[b] Latency time to fall from a thin wire, n=10–12.

[c] Seizure stage (see methods) induced by a subconvulsant dose of pentylenetetrazol (35 mg/kg), n=6–12.

* $p<0.05$,

** $p<0.01$,

*** $p<0.001$.

Table 2

Relative mRNA expression levels of *Gabrb3* in adult heterozygous mice compared to controls.

Genotype	Dorsal root ganglia	Spinal cord	Whole brain
Female			
+/+	1.00 ± 0.12	1.00 ± 0.07	1.00 ± 0.10
p+/m−	0.41 ± 0.13**	0.46 ± 0.12*	0.50 ± 0.05*
p−/m+	0.41 ± 0.17**	0.46 ± 0.04*	0.50 ± 0.06*
Male			
+/+	1.00 ± 0.12	1.00 ± 0.06	1.00 ± 0.04
p+/m−	0.44 ± 0.16**	0.45 ± 0.13*	0.52 ± 0.07**
p−/m+	0.41 ± 0.09**	0.51 ± 0.12*	0.54 ± 0.08**

Data presented as the mean ± SD for six control mice, per gender, and four to six heterozygous mice from each variant. DRG and spinal cord were normalized to the *Hrpt* gene with whole brain samples normalized to the β-actin gene.

* $p<0.05$,

** $p<0.01$ relative to gender-matched controls.